Neurobiology of Aging 54 (2017) 59–70

Contents lists available at ScienceDirect

Neurobiology of Aging

journal homepage: www.elsevier.com/locate/neuaging

Kalirin reduction rescues psychosis-associated behavioral deficits in APPswe/PSEN1dE9 transgenic mice

Josh M. Krivinko [a,1], Susan L. Erickson [a,1], Eric E. Abrahamson [b], Zachary P. Wills [c], Milos D. Ikonomovic [a,b,d], Peter Penzes [e,f], Robert A. Sweet [a,b,g,*,2]

[a] Department of Psychiatry, University of Pittsburgh School of Medicine, Pittsburgh, PA, USA
[b] Department of Neurology, University of Pittsburgh School of Medicine, Pittsburgh, PA, USA
[c] Department of Neurobiology, University of Pittsburgh School of Medicine, Pittsburgh, PA, USA
[d] Geriatric Research, Education, and Clinical Center, VA Pittsburgh Healthcare System, Pittsburgh, PA, USA
[e] Department of Physiology, Northwestern University Feinberg School of Medicine, Chicago, IL, USA
[f] Department of Psychiatry and Behavioral Sciences, Northwestern University Feinberg School of Medicine, Chicago, IL, USA
[g] Mental Illness Research, Education, and Clinical Center, VA Pittsburgh Healthcare System, Pittsburgh, PA, USA

ARTICLE INFO

Article history:
Received 30 July 2016
Received in revised form 18 January 2017
Accepted 9 February 2017
Available online 16 February 2017

Keywords:
Psychosis
Alzheimer disease
Kalirin

ABSTRACT

Psychosis in Alzheimer's disease (AD+P) represents a distinct clinical and neurobiological AD phenotype and is associated with more rapid cognitive decline, higher rates of abnormal behaviors, and increased caregiver burden compared with AD without psychosis. On a molecular level, AD+P is associated with greater reductions in the protein kalirin, a guanine exchange factor which has also been linked to the psychotic disease, schizophrenia. In this study, we sought to determine the molecular and behavioral consequences of kalirin reduction in APPswe/PSEN1dE9 mice. We evaluated mice with and without kalirin reduction during tasks measuring psychosis-associated behaviors and spatial memory. We found that kalirin reduction in APPswe/PSEN1dE9 mice significantly attenuated psychosis-associated behavior at 12 months of age without changing spatial memory performance. The 12-month-old APPswe/PSEN1dE9 mice with reduced kalirin levels also had increased levels of the active, phosphorylated forms of p21 protein (Cdc42/Rac)–activated kinases (PAKs), which function in signaling pathways for maintenance of dendritic spine density, morphology, and function.

Published by Elsevier Inc.

1. Introduction

Psychotic symptoms, delusions and hallucinations, are common in AD subjects (AD with psychosis, AD+P), cause significant distress, and show limited response to existing treatments. Ropacki and Jeste (Ropacki and Jeste, 2005) comprehensively reviewed the literature on psychosis in AD from 1990 to 2003, identifying 55 studies that comprised 9749 subjects. The median prevalence of AD+P was 41% (range = 12.2%–74.1%). Consistent with these observations, we recently estimated the annual incidence of psychosis in AD subjects at ~10% (Weamer et al., 2016). The most rapid increase in the rates of psychosis in AD is in the transition from mild cognitive impairment to early and middle stages of disease, with a plateau in later stages (Lopez et al., 2003; Ropacki and Jeste, 2005; Weamer et al., 2016). When present, psychotic behaviors in AD have an adverse impact on the patient and family. AD+P is associated with greater distress for caregivers and higher rates of institutionalization (Kaufer et al., 1998; Lopez et al., 1999). In addition, psychosis is associated with the presence of additional abnormal behaviors in AD patients, such as aberrant motor behaviors, agitation, and disinhibition (Vilalta-Franch et al., 2010). Efforts to treat psychosis in AD with medications developed to treat similar symptoms in patients without dementia have shown limited efficacy and effectiveness (Schneider et al., 2006), potentially because of the lack of biologic specificity. Moreover, these medications have high toxicity in this age group, with increased risk of all-cause mortality even after short-term treatment (Huybrechts et al., 2012; Schneider et al., 2005).

Ultimately, the development of more specific treatments for AD+P will depend on the identification of biological correlates of this syndrome, and the development of translational models to evaluate them. The occurrence of psychosis within individuals diagnosed with AD is familial (Hollingworth et al., 2007; Sweet et al., 2002, 2010), with an estimated heritability of 61% (Bacanu

* Corresponding author at: Biomedical Science Tower, Rm W-1645, 3811 O'Hara Street, Lothrop and Terrace Streets, Pittsburgh, PA 15213-2593, USA. Tel.: 412-624-0064; fax: 412-624-9910.
E-mail address: sweetra@upmc.edu (R.A. Sweet).
[1] Denotes equal contributions.
[2] http://www.sweetlab.pitt.edu/.

0197-4580/$ – see front matter Published by Elsevier Inc.
http://dx.doi.org/10.1016/j.neurobiolaging.2017.02.006

et al., 2005; Barral et al., 2015), indicating that psychosis in AD has distinct underlying neurobiology. Kalirin is a Rac1/RhoA guanine nucleotide exchange factor with critical roles in dendritic spine maintenance and growth (Rabiner et al., 2005). Kalirin mutations, gene expression, and protein levels have been associated with risk for the psychotic disorder schizophrenia (Deo et al., 2011; Hill et al., 2006; Kushima et al., 2010; Rubio et al., 2012). We, therefore, evaluated kalirin protein levels in the cortex of individuals with AD+P, in comparison to AD subjects without psychotic symptoms and control subjects without dementia (Murray et al., 2012). We found significantly decreased levels of the 3 major kalirin isoforms, kalirin-7, -9, and -12, in patients with AD compared with control subjects, with further reductions of all 3 in AD+P relative to AD−P.

The simplest hypothesis arising from the association of psychosis in AD with reduced kalirin levels is that kalirin reduction modifies AD pathology so as to drive the psychotic phenotype. However, interactions between kalirin and amyloid β (Aβ) have not, to our knowledge, been previously explored in an experimental model. We, therefore, sought to evaluate this hypothesis by reducing kalirin protein levels in mice transgenic for humanized *APP* and *PSEN1* (APPswe/PSEN1dE9), each containing causal mutations for AD (Jankowsky et al., 2004). The APPswe/PSEN1dE9 model demonstrates detectable Aβ deposits by 4 months of age, with increasing levels of soluble and insoluble Aβ up to at least 12 months of age (Izco et al., 2014; Jankowsky et al., 2004). The combined mutations produce $A\beta_{1\text{-}42}$ as the predominant Aβ species resulting in an increased ratio of $A\beta_{1\text{-}42}/A\beta_{1\text{-}40}$ compared with mice transgenic for the *APP*swe mutation alone (Jankowsky et al., 2004). Because individuals with AD+P exhibited moderately decreased levels of kalirin isoforms compared with AD-P and control subjects (Murray et al., 2012), we chose to compare APPswe/PSEN1dE9 mice with normal kalirin levels to those that were heterozygous for kalirin deletion rather than to APPswe/PSEN1dE9 mice completely lacking kalirin.

How to best evaluate psychosis and related behavioral disturbances found in AD subjects in a mouse model is not currently established. A widely used approach derives from the findings that subjects with psychosis due to schizophrenia have sensory impairments, such as reduced habituation and reduced prepulse inhibition (PPI) of the acoustic startle response (ASR), both of which are readily assessed in rodent models (Swerdlow and Geyer, 1998). Other impairments of auditory sensory processing reported in patients with schizophrenia, such as reduced ability to discriminate brief gaps in noise, can also be assayed in the rodent (Moyer et al., 2016). A limited number of studies have evaluated PPI phenotypes in transgenic mouse models of AD pathology with evidence supporting the presence of impairments that increase as age and pathology advance (McCool et al., 2003; Wang et al., 2012). The one study we identified to evaluate habituation of startle, Wang et al., found no effect of genotype on habituation in mice transgenic for human mutant *APP*swe and the *PSEN1* M146L mutation (Wang et al., 2012). To our knowledge, gap detection has not been studied.

In contrast to these limited studies of behaviors associated most directly with psychosis, other behaviors that are frequently comorbid with AD+P, such as increases in motor activity and disinhibition, have been studied extensively in *APP* and *PSEN1* transgenic mice. A recent comprehensive review concluded that despite some conflicting findings, increased hyperactivity in the open field test (OFT) with age was the most common pattern in mice transgenic for the APPswe mutation, including in APPswe/PSEN1dE9 mice, suggesting a relationship to accumulation of pathology (Lalonde et al., 2012). *APP* transgenic mice strains were more variable in demonstrating decreased, increased, or unchanged anxiety/inhibition (Lalonde et al., 2012), although several studies have reported APPswe/PSEN1dE9 mice to evidence disinhibition/reduced anxiety (Dumont et al., 2004; Lalonde et al., 2005; Reiserer et al., 2007).

We, therefore, first undertook to identify which psychosis-associated behaviors were present in APPswe/PSEN1dE9 transgenic mice utilizing a battery of tests: PPI and habituation of acoustic startle, gap detection, OFT, and spontaneous alternation. APPswe/PSEN1dE9 demonstrated reduced habituation to acoustic startle, increased motor activity, and increased disinhibition in comparison with wild-type mice. These tests were then combined in an integrated psychosis-associated behavioral z-score, an analytic approach developed to improve the sensitivity and reliability of behavioral measurement in mouse models (Guilloux et al., 2011). In comparison to APPswe/PSEN1dE9 mice with normal kalirin levels, APPswe/PSEN1dE9 mice with reduced kalirin levels demonstrated the rescue of psychosis-associated behavior between 6 and 12 months. Groups did not differ on cognitive behavior assessed using the radial arm water maze nor on measures of soluble $A\beta_{1\text{-}42}$, APP, or tau levels. Of interest, kalirin reduction in the context of Aβ overproduction was associated with increased levels of phosphorylated PAKs, which function in signaling pathways for maintaining dendritic spine density, morphology, and function.

2. Material and methods

2.1. Mouse models

Presenilin and amyloid precursor protein transgenic mice (APPswe/PSEN1dE9): B6.Cg-Tg(APPswe, PSEN1dE9)85Dbo/Mmjax mice were developed by Dr. David Borchelt, McKnight Brain Institute, University of Florida (Borchelt et al., 1997; Jankowsky et al., 2001). These mice contain 2 transgenes each controlled by a mouse prion promoter and inserted at a single locus between Arpp21 and Pdcd6ip on chromosome 9. The first transgene contains cDNA for a chimeric *APP* in which the mouse sequence encoding the Aβ domain has been replaced with the human sequence for 3 amino acids and with the sequence encoding the human Swedish mutations K595N/M596L. The second transgene contains the cDNA for human *PSEN1* containing the deltaE9 mutation, a deletion of exon 9. Breeding pairs consisting of a APPswe/PSEN1dE9 male and a wild-type female littermate were ordered from the Mutant Mouse Regional Resource Center, University of Missouri (Stock # 034832-JAX). The order was fulfilled by The Jackson Laboratories (JAX, Bar Harbor, ME, USA) with mice congenic on a C57Bl/6J background (generation N17). The line was maintained at the University of Pittsburgh by breeding APPswe/PSEN1dE9 males with wild-type C57Bl/6J females (littermates or purchased from JAX).

Kalirin underexpressors: The construct for deletion of the *KALRN* gene was developed in the laboratory of Dr. Peter Penzes, Northwestern University, by replacing exons 27–28 and the intervening intron with a neo cassette under an independent PGK promoter. Using this construct, mice deficient in kalirin protein were generated from ES cells by inGenious Targeting Laboratory (Ronkonkoma, NY, USA) (Cahill et al., 2009). C57Bl/6NCR mice bearing the targeted deletion were provided to JAX, where they were rederived on a C57Bl/6NJ background and shipped to the University of Pittsburgh. The line was maintained by breeding males heterozygous for the *KALRN* deletion to wildtype C57Bl/6J females (JAX).

APPswe/PSEN1dE9 males were mated to *KALRN*+/− females, yielding 4 genotypes: APPswe/PSEN1dE9/*KALRN*+/+ (APP/PS1/KALRN(+/+)), APPswe/PSEN1dE9/*KALRN*+/− (APP/PS1/KALRN(+/−)), *KALRN*+/+ (KALRN(+/+)), and *KALRN*+/− (KALRN(+/−)). Male pups produced from the *KALRN*+/−, APPswePSEN1dE9 cross were identified with numbered ear tags and genotyped from tail snips collected at postnatal day (P)14, and then weaned into social group housing (2–4 per cage) at P21–23.

2.2. Behavioral testing

Mice were run through a series of behavioral tests at either 5–6 (6m) or 11–12 months of age (12m). Mice from the younger cohort were transported to the testing rooms in their home cages and tested on OFT, spontaneous alternation, and ASR with either noise PPI (ASR/PPI) or gap PPI (ASR/GAP) over a 2-week period. During week 1, mice were transported to the testing room for 30 minutes acclimation on days 1 and 2, OFT on day 3 and spontaneous alternation on day 4. During week 2, mice were acclimated to a different room for about 2 hours and part of the restraint apparatus from the startle chamber was placed in the home cage on day 1. Mice were placed in the startle chambers for 30 minutes on day 2 and then tested on ASR/PPI and ASR/Gap on days 3 and 4, respectively. Mice from the older cohort were placed in individual cardboard buckets and transported to the testing rooms on a cart. This latter group was exposed to the same series of tests as the younger animals, plus an additional week of testing on radial arm water maze (RAWM) and open swim. All equipment except the swimming pools were wiped clean with quatricide followed by water before exposure to each animal and after the last animal for the day. All testing was done with the experimenter blind to genotype.

2.2.1. Open field test (OFT)

Mice were placed in a rectangular arena (43 cm × 43 cm × 30 cm; Med Associates Inc., Fairfax, VT, USA), with a solid floor and an open top, for 30 minutes. The animals' horizontal and vertical movements were monitored with infrared light beams and detectors placed along the sides of the walls of the arena. Movements in the X-Y plane were tracked by beam breaks 2.5 cm above the floor. Rearing behavior (vertical counts) was recorded from beam breaks at 7.5 cm above the floor. Beam interruptions were analyzed with the aid of Med-Associates proprietary software. The innermost 15 × 15 cm square was defined as the center of the arena for analysis, whereas the area outside of this innermost square was defined as the perimeter. The ambient illumination level was 40–45 lux in the center of each chamber. Results are reported for the first 10 minutes.

2.2.2. Spontaneous alternation

Three arms (40 cm × 4.5 cm × 12 cm) of an 8-arm plexiglass radial maze were utilized, and ambient light adjusted to 40–45 lux in each arm. Each mouse was placed at the end of 1 arm and allowed to freely explore the apparatus with the experimenter out of sight. Mouse activity was video-recorded through a camera mounted above the maze. Entries into each arm were hand scored for 10 minutes beginning from the first entry.

2.2.3. Acoustic startle response (ASR)

ASR testing used a previously described protocol (Moyer et al., 2016). Mice were placed in holders in ASR chambers (StartleMonitor, Kinder Scientific, Poway, CA, USA) and acclimated to 65-dB background white noise for 5 minutes. Startle-only trials consisted of short bursts of 75–115 dB white noise. PPI trials consisted of a 40 ms, nonstartling white noise pulse ranging 67–75 dB (2–10 dB above background noise), followed 100 ms later by a 115-dB startle pulse. Mice were exposed to a series of startle-only trials, background-only trials, and PPI trials in 10 blocks of 10 trials each, in a pseudorandomized order, with varying intertrial intervals (Table S1A). Each animal's startle was measured (in Newtons) from the peak response in the 60 ms following the onset of the startle pulse. Blocks of 5 startle-only trials were included at the beginning (reported as ASR [Pre]) and end (reported as ASR [Post]) of each session to assess habituation of startle reflex over the session. Because there were no group differences in ASR (Pre), habituation of the startle response was represented by the mean ASR (Post). ASR/Gap was assessed in the same animals on the following day, using an approach similar to ASR/PPI, but a silent gap (1–250 ms) embedded in 65-dB background noise 100 ms before the startle stimulus served as the prepulse (Table S1B).

2.2.4. Radial arm water maze (RAWM)

The RAWM apparatus was custom made of gray plastic with fixed lanes (Coulbourn Instruments, Whitehall, PA, USA; arm length 455 mm, arm width 75 mm, and center diameter 155 mm.) The pool was filled with tap water (20 °C ± 1 °C) to a level approximately 7 cm below the walls defining the lanes. The water was made opaque with white tempera paint to help conceal the submerged escape platform for hidden platform trials and enhance contrast with the dark coat color of the mice. Conspicuous visual targets were placed around the pool and ambient light was 6 lux. Mice were tested individually, taking turns in groups of 4. Each mouse had 15 trials/day blocked into sets of 6, 6, and 3, with a minimum rest of 5 minutes between trials and 1 hour between sets. If a mouse failed to find the escape platform in 60 seconds, the experimenter guided the mouse to the platform. Once on the platform, each mouse was allowed to rest for 20 seconds to orient. On day 1, consecutive trials for each mouse alternated between visible and hidden platform by attaching or removing a 1-cm thick platform extension with a 10-cm tall black flag attached. On days 2 and 3, the escape platform was hidden for all trials. The target arm was varied for different mice to help reduce olfactory cues. The target arm was constant for a given mouse on days 1 and 2, and then moved 2 arms away for day 3. Start arms varied randomly. The number of entries into incorrect arms (errors) was recorded until the mouse found the escape platform, or for 60 seconds, whichever came first, and the mean number of errors was calculated for blocks of 3 consecutive trials for each animal. Mice were dried with paper towels and returned to their transport buckets placed against a heating pad between trials.

2.2.5. Open swim

To assess the swim speed and visual acuity of the mice, a blue plastic pool (1-m diameter, 0.75-m height) was partially (~1/3) filled with water (20 °C ± 1 °C) made opaque with white tempera paint. This gave the mice a uniform horizon around the perimeter of the pool. The visible escape platform used for RAWM was placed in the center of 1 quadrant. Each mouse was placed into the water in the center of 1 of the other quadrants, facing the pool wall. Mice were allowed to swim until they reached the platform, or for 60 seconds. Each mouse had a total of 15 trials with resting periods as described for RAWM.

2.3. Protein assays

Mice were weighed and deeply anesthetized with Nembutal (150 mg/kg) and transcardially perfused with ice-cold normal saline. Brains were rapidly extracted and bisected. The right cerebral cortex was separated from underlying structures and rapidly frozen.

2.3.1. Western blot

Tissue from the right cerebral cortex was homogenized and sonicated in ice-cold SDS extraction buffer (0.125-M Tris-HCl [pH 7], 2% SDS, and 10% glycerol), followed by centrifugation at 16,100g for 10 minutes. Total protein was extracted using SDS extraction buffer at 70 °C. Protein concentration was estimated using a bicinchoninic acid assay (BCA Protein Assay Pierce # 23,225). Genotype groups were run together and each sample assayed in duplicate. The final protein concentration utilized for each sample was estimated from

the mean of the duplicates. For SDS-PAGE, sets of 4 mice (1 of each genotype) were run together, with 2 lanes per mouse. Protein (12.5 μg) was aliquoted in 1× LI-COR Protein Loading Buffer (Li-Cor #928-40004, Licor Inc., Lincoln, NE, USA), loaded on 4%–20% SDS-PAGE gradient gels (Thermo Scientific #26224, Thermo Scientific, Rockford, IL, USA), and separated for 1.5–2.5 hours at room temperature in 1× SDS running buffer (Pierce 20X Tris Hepes SDS Buffer #28368) at 75 V. Samples were then transferred to polyvinylidene fluoride membranes (Millipore Immobilon-FL PVDF #PFL00010) in 1× Tris Glycine Blotting Buffer (Pierce #28363) at 85 V, for 50 minutes at 4 °C.

Membranes were incubated for 1 hour in Odyssey Li-Cor Blocking Buffer (Li-Cor #927-4000) diluted 1:1 in 1× TBS. The membrane was incubated overnight in primary antibodies directed against the spectrin domain of kalirin (rabbit anti-kalirin spectrin, Millipore #07-122, 1:500); Aβ/APP (mouse anti-Aβ 1-16, Clone 6E10, BioLegend #803001, 1:1000); total tau (mouse anti-tau, clone tau-5, a.a. 210-241, Millipore #MAB361, 1:2000); PAK1/2/3 (rabbit anti-PAK 1/2/3, Cell Signaling Technologies #2604, 1:500), or phospho-PAK (rabbit anti-phospho-PAK1 (Thr423)/PAK2 (Thr402)/PAK3 (Thr421), Cell Signaling Technologies #2601, 1:1000). Each of these antibodies was paired with an anti-β-tubulin primary antibody (1:60,000) as a loading control (either Millipore #05-661, raised in mouse, or Abcam #ab6046, raised in rabbit). Antibodies were diluted in Pierce SuperBlock blocking buffer (Pierce #37353) with 0.1% Tween 20 (Sigma #P7949, Sigma-Aldrich, St. Louis, MO, USA). Membranes were then incubated in LiCor IRDye secondary antibodies (Li-Cor: goat anti-rabbit 800 nm #926-32211; goat anti-mouse 680 nm #926-68020) 1:10,000 in Odyssey Li-Cor Blocking Buffer (Li-Cor #927-4000) diluted 1:1 with TBS (0.1% Tween 20 + 0.02% SDS). Blots were dried and scanned, and bands were detected using a Li-Cor Odyssey Infrared Scanner set at a resolution of 42 μm and the highest image quality. Images were quantified using MCID Core Version 7.0 (InterFocus Imaging Ltd., Linton, Cambridge, UK). The peak for each of the 4 isoforms of kalirin and β-tubulin on the output histograms were independently aligned to a single point on the distance axis for all lanes from all blots. The integrated intensity (mean intensity × number of pixels) was acquired for each protein.

2.3.2. ELISA

Tissue from the right cerebral cortex was homogenized on ice in phosphate-buffered saline (300 mg/mL) and rehomogenized (150 mg/mL) in DEA homogenization buffer (0.2% DEA, 100-mM NaCl, and 10 μL/mL) with Sigma P8340 protease inhibitor cocktail (Sigma-Aldrich, St. Louis, MO, USA). $A\beta_{1\text{-}42}$ peptide concentration was quantified in diethylamine (DEA)-soluble Aβ fractions as described previously (Ikonomovic et al., 2008). The DEA-soluble fraction was prepared by centrifuging the homogenate aliquot at 135,000g at 4 °C for 1 hour and neutralizing the supernatant with 0.5-M Tris-Cl. The pellet was saved for preparing the insoluble fraction. The pellet was resuspended in phosphate-buffered saline and 10 μL/mL Sigma P8340 protease inhibitor cocktail (300 mg/mL), sonicated in 70% formic acid for 1 minute on ice to produce the insoluble Aβ fraction which was then centrifuged at 135,000g at 4 °C for 1 hour, and the supernatant was neutralized with 1-M tris base and 0.5-M Na_2HPO_4. Soluble and insoluble Aβ concentrations were assayed using a colorimetric TMB-based ELISA (Invitrogen, Carlsbad, CA, USA) read at 450 nm, with a capture antibody specific for the NH2 terminus of human Aβ (amino acids 1–16) and detection antibodies specific for the neoepitope at the 42-amino acid end of Aβ. Values were determined from standard curves using synthetic Aβ peptide (Invitrogen, Carlsbad, CA, USA) and are expressed as picomoles per gram wet brain tissue.

2.4. Dissociated neuron cultures

P0 KALRN(+/+) versus KALRN(+/−) mice were sacrificed by rapid decapitation after induced hypothermia. Dissociated cortical neurons from mice were plated onto 18-mm diameter coverslips coated with human laminin overlying a poly-D-lysine layer (neuVitro, Vancouver, WA, USA) at a density of 1.5 million neurons per coverslip using plating media containing 10% donor horse serum (Invitrogen, Carlsbad, CA, USA) in 12-well culture plates. After 3 hours, cultures were maintained in Neurobasal media (Invitrogen, Carlsbad, CA, USA) with B27 supplement (Gibco, Grand Island, NY, USA) for 25 days. On DIV-21, an equal number of culture wells from each mouse pup were exposed to $A\beta_{1\text{-}42}$ peptide (rPeptide, Bogart, GA, USA), which was solubilized in dimethyl sulfoxide with F12 media (Caisson Laboratories, Smithfield, UT, USA), incubated for 24 hours at 4 °C, and used at a final concentration of 1-μM $A\beta_{1\text{-}42}$ per well or an equivalent amount of dimethyl sulfoxide/F12 vehicle. We (unpublished data), and others (Laurén et al., 2009; Nicoll et al., 2013) have shown that this yields soluble oligomeric $A\beta_{1\text{-}42}$. After 48 hours, neurons were re-exposed to the same concentration of $A\beta_{1\text{-}42}$ solution or an equivalent amount of vehicle solution for an additional 48 hours. We have found that this exposure regimen causes reductions in dendritic spine and synapse numbers, and LTP impairments in cultures from wild-type mice (unpublished data). Coverslips were then washed once in 1000-μL Hank's Balanced Salt Solution (HBSS; Gibco, Grand Island, NY, USA) and neurons were scraped into 150-μL ice-cold radioimmunoprecipitation assay (RIPA) buffer (Thermo Scientific, Rockford, IL, USA) with protease and phosphatase inhibitors. Each sample consisted of an equal volume of protein homogenate from 2 separate mouse pups of the same genotype and exposure conditions. Samples were centrifuged at 17,000g for 10 minutes, and protein concentration was estimated in duplicate using bicinchoninic acid assay (Thermo Scientific, Rockford, IL, USA). Samples were prepared for Western blot as described in Section 2.3.1.

2.5. Statistical analysis

Data were analyzed with SPSS using ANOVA. Fixed effects of genotype and, as appropriate, age and genotype by age interaction were tested.

Z-scores for psychosis-associated behavior were modeled after emotionality Z-scores developed to synthesize a single measure from multiple convergent and complementary behavioral assays (Guilloux et al., 2011). For each of the included behaviors, we calculated the mean and standard deviation (SD) of the KALRN(+/+) mice for the 6 months age group. The difference between each individual's score and the KALRN(+/+) mean for the 6 months age group was calculated and divided by the 6 months KALRN(+/+) SD. The direction of the tests was adjusted so that higher scores reflected greater psychosis-associated behavior (Table 1), and the mean of the standardized scores was then calculated for each animal.

Table 1
Behavioral parameters included in summary psychosis-associated behavior z-score

Psychosis-associated behavior	Test	Parameter	Abnormal direction
Aberrant motor behavior	OFT	Total distance	Higher
Aberrant motor behavior	OFT	Perimeter vertical counts	Higher
Aberrant motor behavior	Spontaneous Alternation	Number of arm entries	Higher
Disinhibition	OFT	% Distance in center	Higher
Habituation of startle	ASR	ASR (Post)	Higher

3. Results

3.1. Behavior

3.1.1. Psychosis-associated behaviors

Separate cohorts of mice were used for behavioral assessment at 6 and 12 months. Significant effects of genotype were seen for multiple measures of motor hyperactivity, including OFT total distance, OFT perimeter vertical counts, spontaneous alternation number of arm entries, and ASR (post) (Fig. 1). OFT perimeter vertical counts also demonstrated a significant age × genotype interaction, as counts increased with age in APP/PS1/KALRN(+/+) mice while declining in KALRN(+/+), although these changes were not independently significant. Spontaneous alternation percent correct, which could be seen as a measure of apathetic or perseverative behavior (Lalonde et al., 2012), did not differ between APP/PS1/KALRN(+/+) and KALRN(+/+) mice (data not shown).

A significant age × genotype interaction was also seen for a measure of anxiety/inhibition, the percent of total distance in the center of the open field (Fig. 1B). On this measure, increasing age was associated with decreasing percent total distance in the center in KALRN(+/+) mice, reflecting increasing anxiety/inhibition, whereas the opposite pattern was present in APP/PS1/KALRN(+/+) mice, resulting in a significant age × genotype interaction.

Tests of sensory function revealed a significant difference between APP/PS1/KALRN(+/+) and KALRN(+/+) mice only for the ASR (post) (Fig. 1F). This impairment was present despite no associations of genotype, or of the age × genotype interaction with ASR magnitude, PPI, or gap detection.

We then combined those measures showing significant genotype (APP/PS1/KALRN(+/+) vs. KALRN(+/+)) or age × genotype effects (Fig. 1J, tasks in boldface print) into a summary score of psychosis-associated behavior (Table 1), and evaluated whether kalirin reduction in APP/PS1/KALRN(+/+) mice impacted this score with age (Fig. 2A). Although there were no significant effects of age or genotype in this comparison, there was a significant age × genotype interaction. While APP/PS1/KALRN(+/−) and APP/PS1/KALRN(+/+) groups did not differ at 6 months, at 12 months APP/PS1/KALRN(+/−) mice had a significant reduction in summary score (Mean [SD]; APP/PS1/KALRN(+/+): 1.762 (0.81); APP/PS1/KALRN(+/−): 0.74 (0.56); $F_{(1,12)} = 7.514$, $p = 0.018$). Nevertheless, the summary score remained significantly elevated relative to KALRN(+/+) at both ages in APP/PS1 mice with and without kalirin reduction. In contrast, summary scores in KALRN(+/−) mice did not differ from KALRN(+/+) at either age, and there was no significant age × genotype interaction (Supplemental Fig. 1).

We then directly compared the Z-scores of the APP/PS1/KALRN(+/+) and APP/PS1/KALRN(+/−) groups in the individual tests that comprise the summary score (Fig. 2B–F). Among these individual tests, a genotype effect was significant only for OFT perimeter vertical counts (Fig. 2D). A trend toward significance was found in the interaction between age and genotype for OFT total distance (Fig 2B) and for OFT perimeter vertical counts (Fig 2D).

3.1.2. Cognitive behavior

We sought to determine whether the improvement in psychosis-associated behaviors at 12 months in APP/PS1/KALRN(+/−) versus APP/PS1/KALRN(+/+) mice was reflective of a generalized improvement in brain function. We, therefore, evaluated 12-month-old mice on the RAWM task (Fig. 3). Repeated measures ANOVA for blocks 1–10 (the first 2 days of training) revealed a significant genotype × block interaction ($p = 0.024$). The APP/PS1/KALRN(+/+) mutants made more errors than both KALRN(+/+) and KALRN(+/−) mice (Fig. 3B, $p = 0.014$ and $p = 0.020$, respectively, Dunnett's 2-sided post hoc). APP/PS1/KALRN(+/−) mice did not differ from APP/PS1/KALRN(+/+) mice ($p = 0.259$, Dunnett's 2-sided post hoc).

When the escape platform was moved to a new location on day 3, we noted qualitatively that the mice which performed best on day 2 made the most perseverative errors, repeatedly entering the arm that held the escape platform on days 1 and 2. However, KALRN(+/+) and KALRN(+/−) mutants learned the new platform location readily and were typically making 0–1 errors by block 15. In contrast, the APP/PS1/KALRN(+/+) and APP/PS1/KALRN(+/−) mutants showed little improvement in the ability to find the platform in its new location. By block 15, APP/PS1/KALRN(+/+) and APP/PS1/KALRN(+/−) mice did not differ from each other and still made significantly more errors than KALRN(+/+) mice (Fig. 3C, APP/PS1/KALRN(+/+) and APP/PS1/KALRN(+/−) versus KALRN(+/+), $p = 0.022$ and 0.002, respectively, Dunnett's 2-sided post hoc). These impairments in APP/PS1/KALRN(+/+) and APP/PS1/KALRN(+/−) mice were not due to genotype differences in swimming or vision, as there were no differences among genotypes in the time to find the visible escape platform in the open swim test (data not shown).

3.2. Protein measures

3.2.1. Kalirin, Aβ, and tau

Reductions of ~40% of all 4 of the major isoforms of kalirin were present in KALRN(+/−) and APP/PS1/KALRN(+/−) mice relative to KALRN(+/+) and APP/PS1/KALRN(+/+) mice at 6 and 12 months (Fig. 4A–C). Kalirin levels were not altered by the presence of the APPswe/PSEN1dE9 transgenes, as APP/PS1/KALRN(+/+) mice did not differ from KALRN(+/+), and APP/PS1/KALRN(+/−) mice were not different from KALRN(+/−) mice at either age. Conversely, kalirin reduction was not associated with any significant change in levels of APP, soluble, or insoluble $A\beta_{1\text{-}42}$ (Fig. 4D–G). Reductions in total tau levels in APP transgenic mice have been reported to protect against elevations in psychosis-associated behaviors and impairments in cognitive behaviors (Roberson et al., 2007). Total tau in mice 12 months of age was unaltered by kalirin reduction (Fig. 4H and I). Consistent with the lack of difference between APP/PS1/KALRN(+/−) and APP/PS1/KALRN(+/+) mice on measures of APP, $A\beta_{1\text{-}42}$, and tau, mortality was not different between these 2 genotypes, although both had increased mortality rates in comparison to KALRN(+/+) mice (Supplemental Fig. 2).

3.2.2. PAK

Activated type I PAKs (PAK1, PAK2, and PAK3) signal downstream of kalirin and have been reported to be reduced in AD, in APPswe transgenic mice, and to contribute to cognitive impairments (Zhao et al., 2006). Although all 4 kalirin isoforms can activate type I PAKs via Rac1 (Ha et al., 2015), kalirin-9, and kalirin-12 also activate RhoA which can antagonize Rac1 activity (Nakamura, 2013). In addition, multiple pathways other than kalirin signaling via Rac1 can activate type I PAKs (Bokoch, 2003), some of which might undergo compensatory alterations in the context of reduced kalirin. Thus, the net effect of genetic reductions in kalirin on PAK activation is difficult to predict and has not been previously examined, either in isolation or in the presence of Aβ. To measure phospho-PAK (p-PAK) levels, we used a phospho-specific antibody which recognizes PAK1, PAK2, and PAK3 only when phosphorylated at residues implicated in engagement of kinase activity, Thr423, Thr402, and Thr421, respectively (Fig. 5C). We then normalized these p-PAK levels to total PAK levels (reported as p-PAK: Total PAK), using an antibody which recognizes total levels of PAK 1, 2, and 3 (Fig. 5A and B). We found that the total levels of type I PAK were unaltered, but p-PAK levels were significantly increased in cerebral cortex homogenates of APP/PS1/KALRN(+/−) mice compared with KALRN(+/+) mice (Fig. 5D, $p = 0.04$, Tukey's test). In

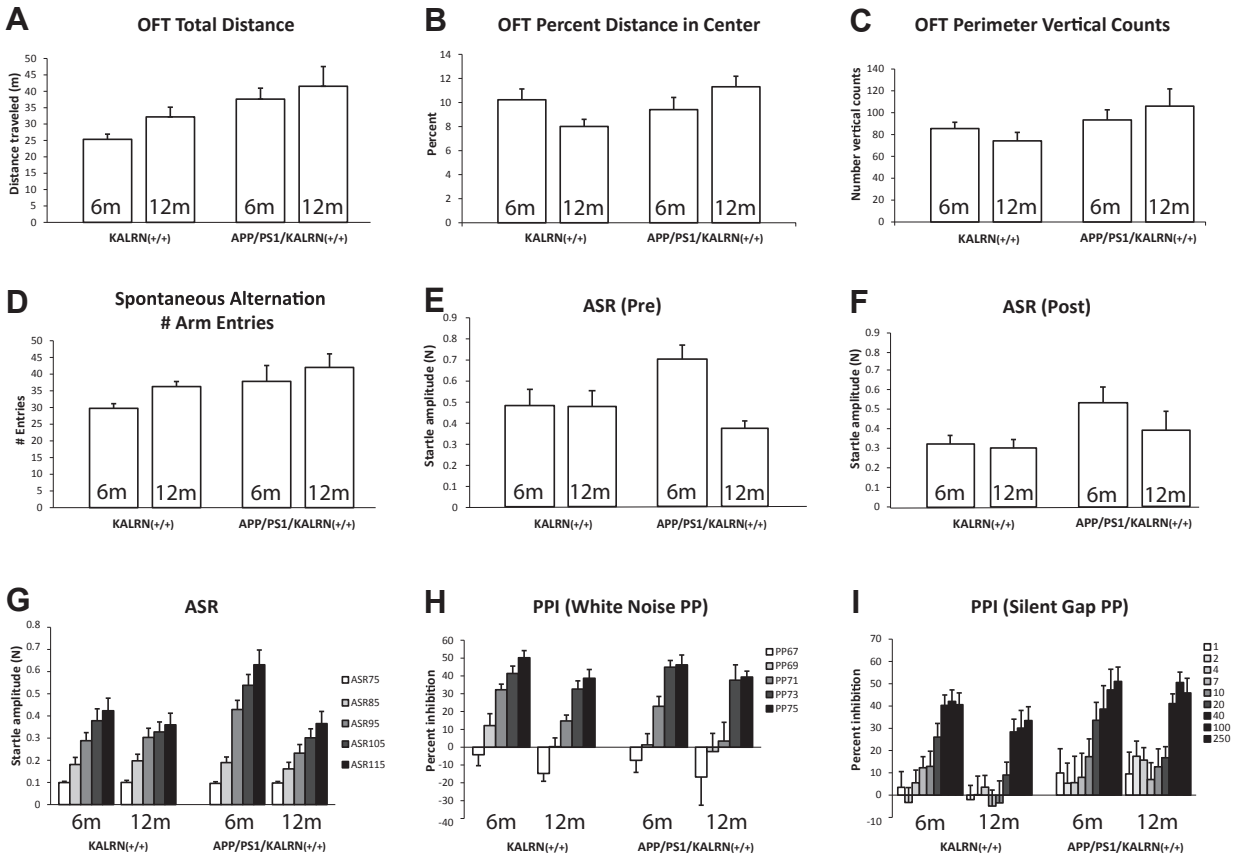

J		ANOVA								
		Age			Genotype			Age x Genotype		
Panel	Task	F	df	Sig.	F	df	Sig.	F	df	Sig.
A	**OFT Total Distance**	7.905	1,47	.007	**30.42**	**1,47**	**<.001**	1.328	1,47	.255
B	**OFT Percent Distance in Center**	.024	1,47	.878	2.630	1,47	.112	**6.405**	**1,47**	**.015**
C	**OFT Perimeter Vertical Counts**	.628	1,47	.432	**13.462**	**1,47**	**.001**	**7.238**	**1,47**	**.01**
D	**Spontaneous Alternation # Arm Entries**	5.045	1,46	.03	**8.535**	**1,46**	**.005**	.001	1,46	.980
E	ASR (Pre)	3.336	1,46	.074	.908	1,46	.346	2.817	1,46	.100
F	**ASR (Post)**	1.175	1,46	.284	**6.892**	**1,46**	**.012**	.493	1,46	.486
G	ASR	2.564	1,46	.041	1.952	1,46	.106	1.128	1,46	.360
H	PPI (White Noise PP)	3.058	1,42	.019	1.729	1,42	.149	.352	1,42	.878
I	PPI (Silent Gap PP)	2.161	1,38	.048	.619	1,38	.773	.448	1,38	.900

Fig. 1. OFT, spontaneous alternation, ASR, habituation of ASR, PPI, and gap detection in 6-month (6m) and 12-month (12m) APP/PS1/KALRN(+/+) and KALRN(+/+) mice. APP/PS1/KALRN(+/+) mice exhibit greater psychosis-associated behavior compared with KALRN(+/+) at both 6m and 12m of age as measured by total distance (A) and perimeter vertical counts (C) in OFT, number of arm entries in spontaneous alternation (D), and ASR (post) (F). Psychosis-associated behavior was exacerbated at 12m as compared with 6m in APP/PS1/KALRN(+/+) mice as measured by percent distance in center (B) and perimeter vertical counts (C) in OFT. There were no significant differences between genotypes or age groups in the ASR (pre) (E), ASR (G), or PPI of the ASR with white noise (H) or silent gap (I). ANOVA results for the contrasts of age, genotype, and age × genotype are included in the table below; significant results are in boldface (J). The number of mice (n) for each genotype and age is as follows KALRN(+/+): 6m n = 16 and 12m n = 17; APP/PS1/KALRN(+/+): 6m n = 11 (for all panels except A, B, and C; n = 12) and 12m n = 7. Error bars represent standard error of the mean (SEM).

contrast to our findings in cortical homogenates, in dissociated primary cortical neuron cultures from KALRN(+/−) mice, exposure to oligomeric Aβ did not increase p-PAK in comparison with either oligomeric Aβ- or vehicle-exposed cultures from KALRN(+/+) mice (Fig 5E and F). However, p-PAK levels were increased in vehicle-exposed cultures from KALRN(+/−) mice relative to KALRN(+/+) mice (Fig. 5E, $p = 0.045$, Fisher's test).

4. Discussion

We undertook, in APPswe/PSEN1dE9 transgenic mice, to determine whether the reductions in kalirin levels we had observed previously in AD+P subjects in comparison with AD subjects (Murray et al., 2012) might modify the expression of psychosis-associated behaviors. To accomplish this goal, we first sought to identify which among a set of

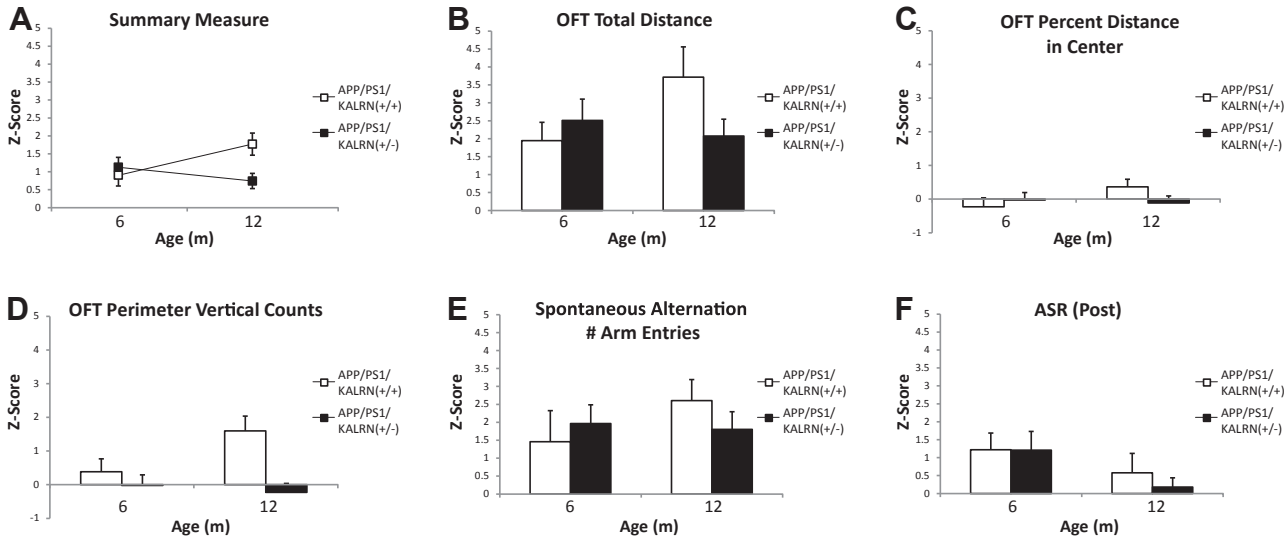

G

		ANOVA								
		Age			Genotype			Age x Genotype		
Panel	Task	F	df	Sig.	F	df	Sig.	F	df	Sig.
A	**Summary**	.626	1,37	.434	1.741	1,37	.196	**4.236**	**1,37**	**.047**
B	OFT Total Distance	1.086	1,38	.304	.708	1,38	.406	2.955	1,38	.094
C	OFT Percent Distance in Center	.931	1,38	.341	.291	1,38	.593	1.703	1,38	.200
D	**OFT Perimeter Vertical Counts**	1.719	1,38	.198	**8.450**	**1,38**	**.006**	3.417	1,38	.073
E	Spontaneous Alternation # Arm Entries	.482	1,37	.492	.044	1,37	.836	.855	1,37	.362
F	ASR (Post)	2.613	1,37	.115	.142	1,37	.709	.128	1,37	.723

Fig. 2. Kalirin reduction attenuates psychosis-associated behavior in 12-month (12m) APP/PS1/KALRN(+/+) mice. Analysis of mean Z-scores generated from APP/PS1/KALRN(+/+) and APP/PS1/KALRN(+/−) mice reveals a significant reduction in psychosis-associated behavior in 12m APP/PS1/KALRN(+/−) mice when compared with 12m APP/PS1/KALRN(+/+) mice (A). Individual measures, including total distance (B), and percent distance in center (C) in OFT, number of arm entries in spontaneous alternation (E), and ASR (post) (F) did not significantly differ between APP/PS1/KALRN(+/+) and APP/PS1/KALRN(+/−) mice. Perimeter vertical counts in OFT were significantly increased in APP/PS1/KALRN(+/+) compared with APP/PS1/KALRN(+/−) mice. ANOVA results for the contrasts of age, genotype, and age × genotype are included in the table; significant results are in boldface (G). The n for each genotype and age is as follows: APP/PS1/KALRN(+/+): 6m n = 11 (for all panels except B, C, D; n = 12) and 12m n = 7; APP/PS1/KALRN(+/−): 6m n = 13 and 12m n = 7. Error bars indicate SEM.

psychosis-associated behaviors were present in this model during the time frame in which progressive pathology develops and cognitive functions are impaired. We found significant increases in aberrant motor behavior and disinhibition, and reduced habituation of ASRs, in 6–12-month-old APPswe/PSEN1dE9 mice. We combined these measures into a summary score of psychosis-associated behavior. This approach has been shown to enhance the power to detect changes in behaviorally complex neuropsychiatric phenotypes as the converging results from multiple, complementary tests reduces variability of the summary measure relative to individual tests (Guilloux et al., 2011). We then evaluated the effect of kalirin reduction in APPswe/PSEN1dE9 transgenic mice on the summary measure of psychosis-associated behavior and found a significant genotype × age interaction. APPswe/PSEN1dE9 transgenic mice with 2 kalirin alleles did not differ in psychosis-associated behavior from APPswe/PSEN1dE9 transgenic mice with only 1 kalirin allele at 6 months, but by 12 months the APPswe/PSEN1dE9 mice with reduced kalirin also had a significant reduction in psychosis-associated behavior. Finally, we found that the behavioral rescue at 12 months was not due to the effects of kalirin reduction on overproduction of human APP or $A\beta_{1\text{-}42}$, or to altered levels of tau. However, kalirin reduction in APPswe/PSEN1dE9 transgenic mice led to an increase in p-PAK1/2/3, a finding not recapitulated by short-term exposure to soluble oligomeric Aβ in vitro.

Several caveats deserve discussion. We chose to combine into the summary score only those behaviors, from among the a priori list of possible psychosis-related behaviors we assessed, that had evidence of disruption in APPswe/PSEN1dE9 transgenic mice. This may have potentially biased us toward detecting lower levels of these behaviors in APP/PS1/KALRN(+/−) mice, via a regression toward the mean. However, such an effect would not readily explain the age-dependent pattern we observed, in which APP/PS1/KALRN(+/−) mice had levels of psychosis-associated behavior similar to the levels observed in APP/PS1/KALRN(+/+) mice at 6 months, but significantly lower than in APP/PS1/KALRN(+/+) mice at 12 months. In addition, we tested separate 6-month and 12-month cohorts of mice. We were able to exclude a possible source of bias, differential survival of APP/PS1/KALRN(+/−) and APP/PS1/KALRN(+/+) mice. Nevertheless, it is possible that the behavioral improvements we observed reflect some other unmeasured factor related to group membership. Firmly concluding that kalirin reduction protects against progressive worsening of psychosis-associated behaviors in APPswe/PSEN1dE9 transgenic mice will require longitudinal testing of individual animals.

Another important caveat is that Aβ overproducing mice used in the present study have relatively limited p-Tau pathology (Kempf et al., 2016; Roberson et al., 2007). Despite the lack of p-Tau

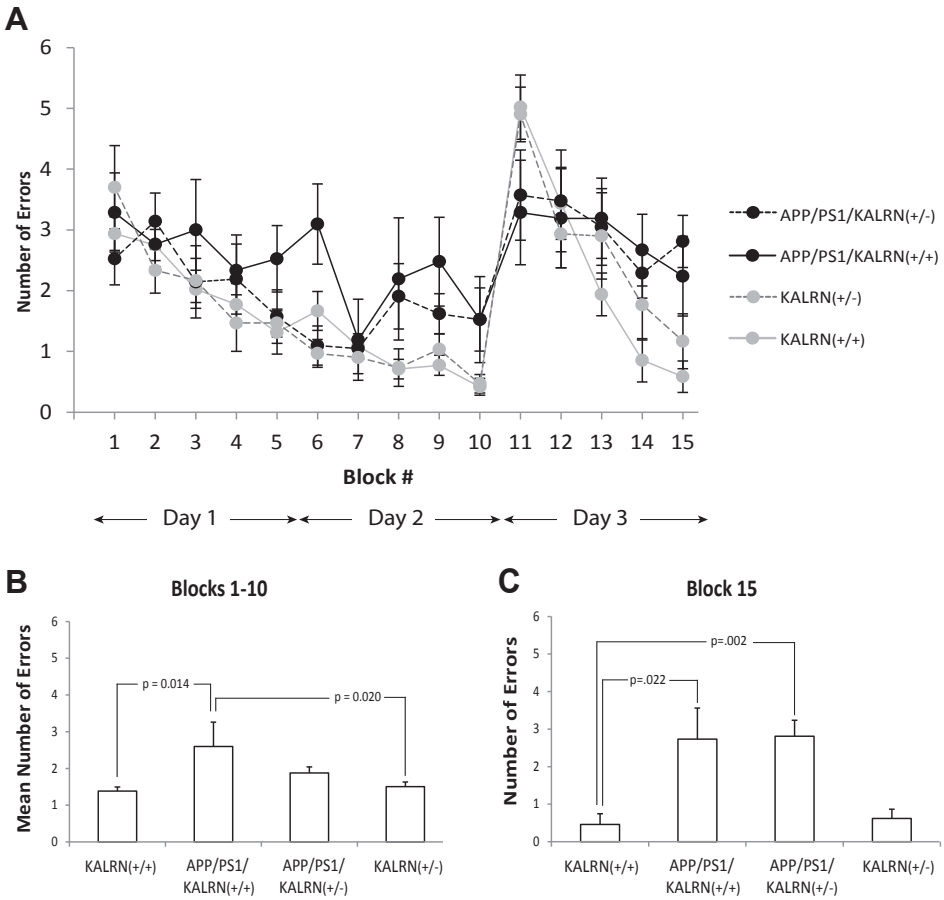

Fig. 3. Performance on RAWM. In blocks 1–10, APP/PS1/KALRN(+/+) mice exhibited significantly impaired ability to find the hidden platform as compared with KALRN(+/+) and KALRN(+/−) mice (A, B). APP/PS1 mice with kalirin reduction did not significantly differ from APP/PS1/KALRN(+/+) mice in mean number of errors during these blocks (B). On day 3, the platform was moved to a new location. APP/PS1/KALRN(+/+) and APP/PS1/KALRN(+/−) mice again did not differ from each other in mean number of errors by Block 15, and both of these groups made more errors than KALRN(+/+) mice (C). The n for each genotype is as follows: KALRN(+/+) n = 16, APP/PS1/KALRN(+/+) n = 7, APP/PS1/KALRN(+/−) n = 7, and KALRN(+/−) n = 10. Error bars indicate SEM.

accumulation in these models, reduction of total tau protects against hyperactive behavior (Roberson et al., 2007). Although such a mechanism did not explain the improved behavior in our APP/PS1/KALRN(+/−) mice, AD+P is associated with increased p-Tau, but not total tau, in comparison with AD subjects without psychosis (Farber et al., 2000; Koppel et al., 2014a; Mukaetova-Ladinska et al., 1995; Murray et al., 2014a). One alternative is a mouse model containing a tau mutation, P301L, associated with frontotemporal dementia. These mice have elevated p-Tau, and have recently been shown to have deficits in PPI that correlate with insoluble p-Tau levels (Koppel et al., 2014b). So called "triple transgenic" mouse models that in addition to *APP* and *PSEN1* mutations contain the P301L mutation may thus represent a compelling model for future tests of the effects of kalirin reduction.

In contrast to the protection against progressive increases in psychosis-associated behaviors seen when kalirin was reduced in APPswe/PSEN1dE9 mice, kalirin reduction was not associated with reduction in psychosis-associated behaviors in mice lacking the APPswe/PSEN1dE9 transgenes. Thus, our data suggest the mechanism of rescue was not via a simple additive genetic effect, but instead that kalirin reduction modified the effects of the APPswe/PSEN1dE9 mutations on psychosis-associated behaviors. It has previously been shown that Rac1, a primary target of kalirin, targets the promoter region of native *App*, increasing transcription, and Rac1 inhibition or knockdown reduces transcription (Wang et al., 2009). Such an effect on mouse *App* could theoretically lower total APP (and subsequently Aβ levels) in our APP/PS1/KALRN(+/−) mice. Mouse Aβ is deposited in plaques in APPswe/PSEN1dE9 transgenic mice (van Groen et al., 2006). However, the magnitude of such an effect is anticipated to be small. For example, in 24-month-old transgenic mice that overexpress the London mutation of human *APP*, mouse $A\beta_{1\text{-}40}$ deposits were less than 1/50th of the amount of human $A\beta_{1\text{-}40}$ deposits and mouse $A\beta_{1\text{-}42}$ deposits were less than 1/10th of the corresponding amount of human $A\beta_{1\text{-}42}$ deposited (Pype et al., 2003). Further, it is unclear how such an effect could lead to lower mean z-score in the APP/PS1/KALRN(+/−) mice between 6 months and 12 months of age, especially since during that time frame we observed a 4–5 fold increase in soluble and insoluble human $A\beta_{1\text{-}42}$ in APP/PS1/KALRN(+/−) mice. Thus, it seems reasonable to conclude that the observed behavioral rescue did not result from the prevention of the acceleration of Aβ accumulation present during this age range.

Alzheimer's disease subjects with psychosis have greater and more rapid cognitive deterioration than Alzheimer's disease subjects without psychosis (Murray et al., 2014b). However, the impairments in the psychotic subjects are largely limited to neocortical-dependent functions and separate from hippocampal-dependent cognitive functions, such as learning and memory, which are equally impaired in both groups (Koppel et al., 2012, 2014c; Paulsen et al., 2000; Perez-Madrinan et al., 2004). Like humans, APPswe/PSEN1dE9 transgenic mice accumulate Aβ in both hippocampus and cerebral cortex. Our observation that kalirin

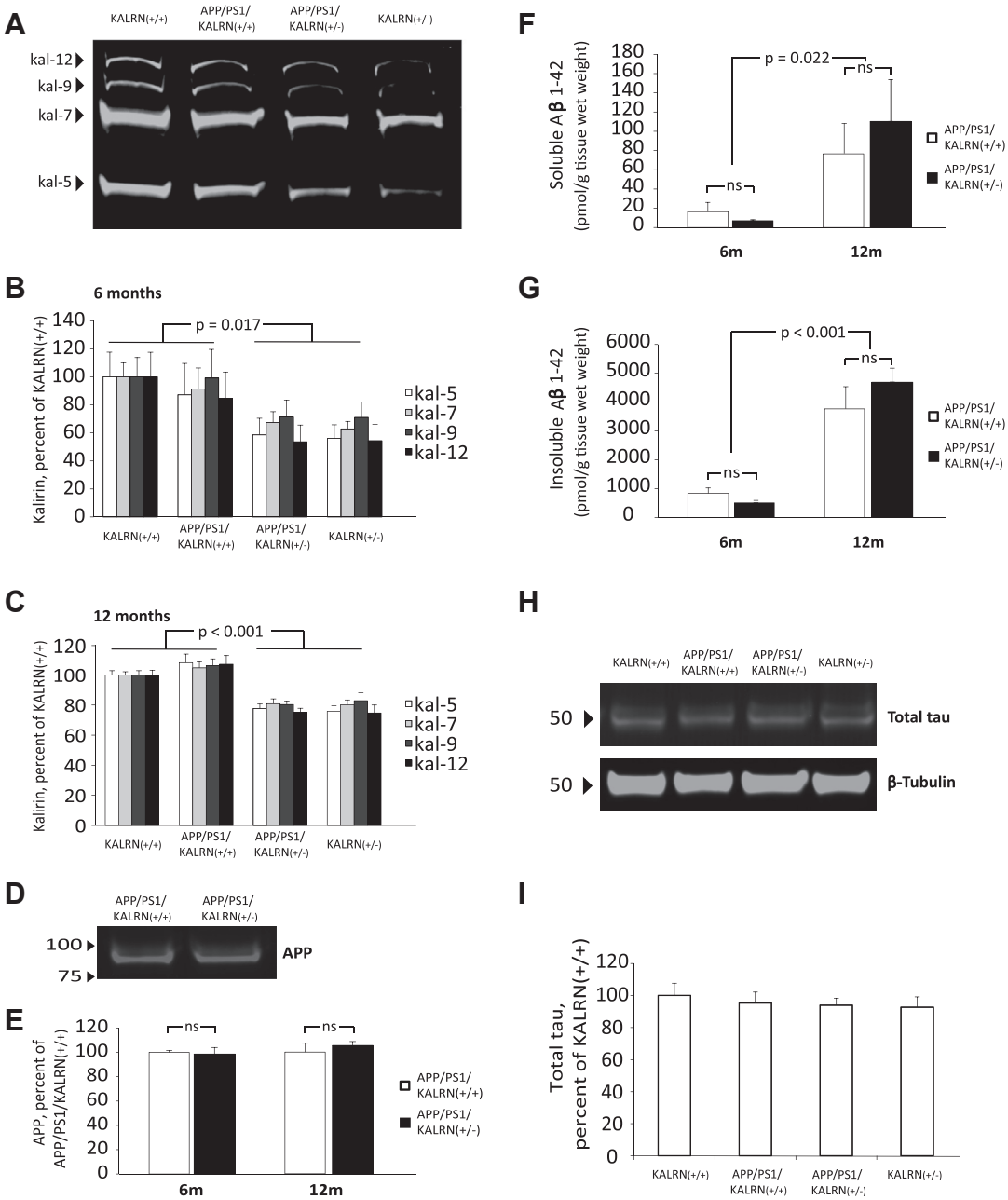

Fig. 4. Levels of kalirin, APP, soluble, and insoluble A$\beta_{1\text{-}42}$, and tau in APP/PS1/KALRN(+/+) and APP/PS1/KALRN(+/−) mice. Representative Western blot of kalirin levels in KALRN(+/+), APP/PS1/KALRN(+/+), APP/PS1/KALRN(+/−), and KALRN(+/−) mice (A). Bands represent 4 different kalirin isoforms, each of which was quantified by optical densitometry, normalized to beta-tubulin intensity as a loading control, and expressed as percent of KALRN(+/+) levels. Levels of all isoforms of kalirin were reduced in both 6-month (6m) and 12-month (12m) APP/PS1/KALRN(+/−) and KALRN(+/−) mice when compared with KALRN(+/+) and APP/PS1/KALRN(+/+) mice. There was no difference in kalirin levels between APP/PS1/KALRN(+/+) and KALRN(+/+) mice at either age or for any kalirin isoform (B, C). The n for each genotype is as follows: KALRN(+/+): 6m n = 8 and 12m n = 16; APP/PS1/KALRN(+/+): 6m n = 8 and 12m n = 7; APP/PS1/KALRN(+/−): 6m n = 8 and 12m n = 7; and KALRN(+/−): 6m n = 8 and 12m n = 10. Representative Western blot of APP in APP/PS1/KALRN(+/+) and APP/PS1/KALRN(+/−) mice (D). APP/PS1/KALRN(+/−) mice did not differ from APP/PS1/KALRN(+/+) mice in levels of APP at either age after normalizing within age groups to percent of APP/PS1/KALRN(+/+). The n for each genotype is as follows: 6m n = 8 per genotype; 12m n = 7 per genotype (E). Levels of soluble (F) and insoluble (G) A$\beta_{1\text{-}42}$ increased from 6m to 12m for both APP/PS1/KALRN(+/+) (n = 6 and n = 7, respectively) and APP/PS1/KALRN(+/−) (n = 4 and n = 7, respectively) mice, whereas levels were not significantly different between genotypes at either time point. Representative Western blots of total tau and beta-tubulin (H). Total tau protein levels were unchanged across all 4 genotypes at 12 months of age (I). The n for each genotype is as follows: KALRN(+/+) n = 9, APP/PS1/KALRN(+/+) n = 7, APP/PS1/KALRN(+/−) n = 7, and KALRN(+/−) n = 9. Error bars represent SEM.

reduction led to an improvement in psychosis-associated behaviors without a concomitant improvement in the hippocampal-dependent RAWM would be consistent with the observations dissociating these functions in human subjects with Alzheimer's disease and psychosis. It is also consistent with prior observations of the effects of kalirin knockout, which leads to reductions in dendritic spine density and Rac1 activation in cerebral cortex, but not in hippocampus, presumably due to the compensation in hippocampus by other guanine nucleotide exchange factors (Cahill et al., 2009).

If not a result of improved hippocampal function, it is worth considering whether the behavioral improvements in APP/PS1/KALRN(+/−) mice might reflect the effects of kalirin reduction in cerebral cortex or elsewhere in the brain. We found increased levels

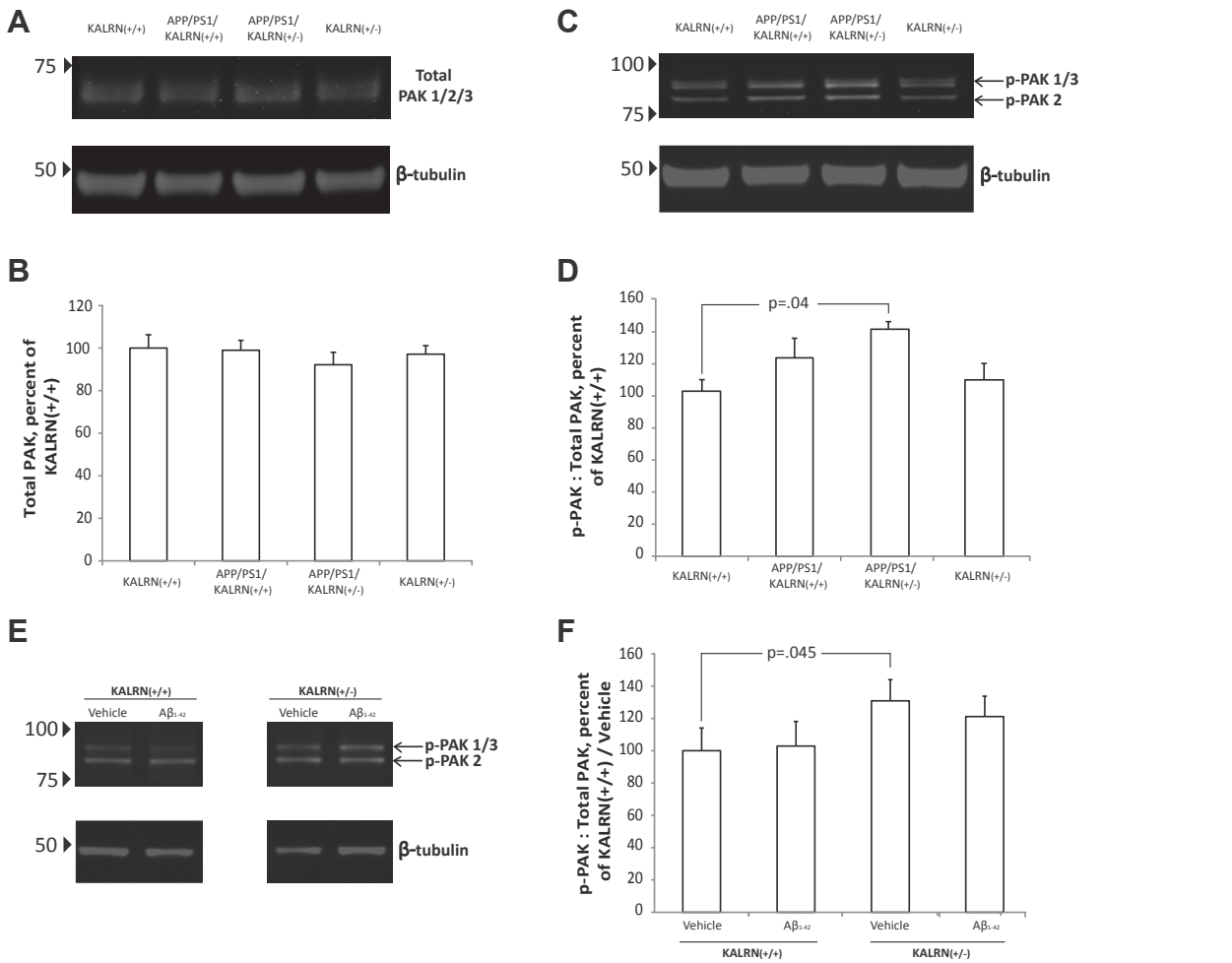

Fig. 5. p-PAK levels in KALRN(+/+) and KALRN(+/−) mice. Representative Western blot of total and phosphorylated type I PAKs (p-PAK) in KALRN(+/+), APP/PS1/KALRN(+/+), APP/PS1/KALRN(+/−), and KALRN(+/−) mice (A, C). Multiple p-PAK bands represent p-PAK 1/3 (upper band) and p-PAK 2 (lower band). Kalirin reduction in the context of Aβ overexpression is associated with a significant increase in p-PAK compared with KALRN(+/+), but no change in total PAK levels (B, D). The n for each genotype in A–D is as follows: KALRN(+/+) n = 9, APP/PS1/KALRN(+/+) n = 7, APP/PS1/KALRN(+/−) n = 7, and KALRN(+/−) n = 9. Representative Western blot of p-PAK levels in primary neuronal culture from KALRN(+/+) and KALRN(+/−) mice, after exposure to $A\beta_{1\text{-}42}$ or vehicle (E). p-PAK levels were increased in KALRN(+/−) mice (F). The n for each group is as follows: KALRN(+/+)/vehicle, n = 4, KALRN(+/+)/$A\beta_{1\text{-}42}$ n = 4, KALRN(+/−)/Vehicle n = 4, and KALRN(+/−)/$A\beta_{1\text{-}42}$ n = 6. Error bars represent SEM.

of activated type-1 PAKs in cerebral cortex in APP/PS1/KALRN(+/−) mice. However, our composite measure of psychosis-associated behaviors comprised a number of functions—increased motor activity, stereotypes, and startle habituation that depend on brainstem structures. Another APPswe/PSEN1dE9 transgenic mouse line has been shown to develop monoaminergic axonopathy, without cell loss, between 4 and 12 months of age, but in that study mice still had locomotor activity at 12 months (Liu et al., 2008). Thus, it seems unlikely that monoaminergic axon die-back accounts for the disturbances in activity we observed. In contrast, combined knockout of *Pak1* and *Pak3* has been shown to result in abnormal dendritic spine morphology in the cerebral cortex and hippocampus, reduced numbers, but enhanced potency, of the remaining synapses, and motor hyperactivity in the OFT (Huang et al., 2011). More recently, it has been demonstrated that forebrain pyramidal neuron selective deletion of ArpC3, a subunit of the Arp 2/3 complex that regulates dendritic spine actin (and is itself a downstream target of PAK signaling (Vadlamudi et al., 2004)), is sufficient to induce abnormal motor behaviors and impairments of PPI (Kim et al., 2013).

We note that our findings of elevated cortical p-PAK levels in APP/PS1/KALRN(+/−) mice were not recapitulated after short-term exposure to Aβ in an in vitro model system. It is not established how to best mimic the sustained Aβ exposure which occurs over the course AD in an in vitro setting. The chronicity of Aβ deposition may be particularly relevant for studying Aβ's effects on p-PAK levels, since previous studies have indicated that levels of p-PAKs in human subjects is dependent on Braak stage (Nguyen et al., 2008). However, the discrepancy between the in vivo and in vitro findings could also indicate that the increases we observed in vivo result from the interaction between kalirin reduction and the effects of the mutations in *APP* and *PSEN1* that are not related to Aβ accumulation.

Further studies will be required to determine whether p-PAK levels may be modifying psychosis-associated behavior in APP/PS1/KALRN(+/−) mice, and whether these changes in p-PAK levels are dependent on PAK's role in influencing dendritic spine morphology and dynamics via ARP2/3 signaling. Investigating these molecular mechanisms may have significance in addition to that for psychosis in AD and schizophrenia, considering human genetic research has identified mutations in PAK3 that lead to variants of X-linked intellectual disability associated with psychotic behaviors (Gedeon et al., 2003; Rejeb et al., 2008). Description of the behavioral and associated morphologic changes may provide insight into the role of the kalirin-PAK pathway in generating psychosis-associated behaviors in neuropsychiatric disease.

Disclosure statement

The authors have no actual or potential conflicts of interest.

Acknowledgements

The authors would like to thank Dr. Patrick Murray for his input on the design of the experiments and Dr. Floh Thiels for her input on the behavioral test battery. All behavioral testing was conducted in the Rodent Behavioral Assessment Core in the Department of Neurobiology at the University of Pittsburgh. This work was supported by grants BX000452 (R. A. S.), MH071533 (R. A. S.), AG014449 (M. D. I.), MH071316 (P. P.), MH097216 (P. P.), and MH107966 (Z. W.). The content is solely the responsibility of the authors and does not necessarily represent the official views of the National Institute of Mental Health, the National Institutes of Health, the Department of Veterans Affairs, or the United States Government.

Appendix A. Supplementary data

Supplementary data associated with this article can be found, in the online version, at http://dx.doi.org/10.1016/j.neurobiolaging.2017.02.006.

References

Bacanu, S.A., Devlin, B., Chowdari, K.V., DeKosky, S.T., Nimgaonkar, V.L., Sweet, R.A., 2005. Heritability of psychosis in Alzheimer disease. Am. J. Geriatr. Psychiatry 13, 624–627.

Barral, S., Vardarajan, B.N., Reyes-Dumeyer, D., Faber, K.M., Bird, T.D., Tsuang, D., Bennett, D.A., Rosenberg, R., Boeve, B.F., Graff-Radford, N.R., Goate, A.M., Farlow, M., Lantigua, R., Medrano, M.Z., Wang, X., Kamboh, M.I., Barmada, M.M., Schaid, D.J., Foroud, T.M., Weamer, E.A., Ottman, R., Sweet, R.A., Mayeux, R., 2015. Genetic variants associated with susceptibility to psychosis in late-onset Alzheimer's disease families. Neurobiol. Aging 36, 3116.e9–3116.e16.

Bokoch, G.M., 2003. Biology of the p21-activated kinases. Annu. Rev. Biochem. 72, 743–781.

Borchelt, D.R., Ratovitski, T., Van Lare, J., Lee, M.K., Gonzales, V., Jenkins, N.A., Copeland, N.G., Price, D.L., Sisodia, S.S., 1997. Accelerated amyloid deposition in the brains of transgenic mice coexpressing mutant presenilin 1 and amyloid precursor proteins. Neuron 19, 939–945.

Cahill, M.E., Xie, Z., Day, M., Photowala, H., Barbolina, M.V., Miller, C.A., Weiss, C., Radulovic, J., Sweatt, J.D., Disterhoft, J.F., Surmeier, D.J., Penzes, P., 2009. Kalirin regulates cortical spine morphogenesis and disease-related behavioral phenotypes. Proc. Natl. Acad. Sci. U. S. A. 106, 13058–13063.

Deo, A.J., Cahill, M.E., Li, S., Goldszer, I., Henteleff, R., Vanleeuwen, J.E., Rafalovich, I., Gao, R., Stachowski, E.K., Sampson, A.R., Lewis, D.A., Penzes, P., Sweet, R.A., 2011. Increased expression of Kalirin-9 in the auditory cortex of schizophrenia subjects: its role in dendritic pathology. Neurobiol. Dis. 45, 796–803.

Dumont, M., Strazielle, C., Staufenbiel, M., Lalonde, R., 2004. Spatial learning and exploration of environmental stimuli in 24-month-old female APP23 transgenic mice with the Swedish mutation. Brain Res. 1024, 113–121.

Farber, N.B., Rubin, E.H., Newhouse, P.A., Kinscherf, D.A., Miller, J.P., Morris, J.C., Olney, J.W., McKeel, D.W., 2000. Increased neocortical neurofibrillary tangle density in subjects with Alzheimer's disease. Arch. Gen. Psychiatry 57, 1165–1173.

Gedeon, A.K., Nelson, J., Gecz, J., Mulley, J.C., 2003. X-linked mild non-syndromic mental retardation with neuropsychiatric problems and the missense mutation A365E in PAK3. Am. J. Med. Genet. A. 120A, 509–517.

Guilloux, J.P., Seney, M., Edgar, N., Sibille, E., 2011. Integrated behavioral z-scoring increases the sensitivity and reliability of behavioral phenotyping in mice: relevance to emotionality and sex. J. Neurosci. Methods 197, 21–31.

Ha, B.H., Morse, E.M., Turk, B.E., Boggon, T.J., 2015. Signaling, regulation, and specificity of the type II p21-activated kinases. J. Biol. Chem. 290, 12975–12983.

Hill, J.J., Hashimoto, T., Lewis, D.A., 2006. Molecular mechanisms contributing to dendritic spine alterations in the prefrontal cortex of subjects with schizophrenia. Mol. Psychiatry 11, 557–566.

Hollingworth, P., Hamshere, M.L., Holmans, P.A., O'Donovan, M.C., Sims, R., Powell, J., Lovestone, S., Myers, A., Devrieze, F.W., Hardy, J., Goate, A., Owen, M., Williams, J., 2007. Increased familial risk and genomewide significant linkage for Alzheimer's disease with psychosis. Am. J. Med. Genet. B Neuropsychiatr. Genet. 144B, 841–848.

Huang, W., Zhou, Z., Asrar, S., Henkelman, M., Xie, W., Jia, Z., 2011. p21-Activated kinases 1 and 3 control brain size through coordinating neuronal complexity and synaptic properties. Mol. Cell Biol. 31, 388–403.

Huybrechts, K.F., Gerhard, T., Crystal, S., Olfson, M., Avorn, J., Levin, R., Lucas, J.A., Schneeweiss, S., 2012. Differential risk of death in older residents in nursing homes prescribed specific antipsychotic drugs: population based cohort study. BMJ 344, e977.

Ikonomovic, M.D., Klunk, W.E., Abrahamson, E.E., Mathis, C.A., Price, J.C., Tsopelas, N.D., Lopresti, B.J., Ziolko, S., Wenzhu, B., Paljug, W.R., Debnath, M.L., Hope, C.E., Isanski, B.A., Hamilton, R.L., DeKosky, S.T., 2008. Post-mortem correlates of in vivo PiB-PET amyloid imaging in a typical case of Alzheimer's disease. Brain 31, 1630–1645.

Izco, M., Martinez, P., Corrales, A., Fandos, N., Garcia, S., Insua, D., Montanes, M., Perez-Grijalba, V., Rueda, N., Vidal, V., Martinez-Cue, C., Pesini, P., Sarasa, M., 2014. Changes in the brain and plasma Abeta peptide levels with age and its relationship with cognitive impairment in the APPswe/PS1dE9 mouse model of Alzheimer's disease. Neuroscience 263, 269–279.

Jankowsky, J.L., Fadale, D.J., Anderson, J., Xu, G.M., Gonzales, V., Jenkins, N.A., Copeland, N.G., Lee, M.K., Younkin, L.H., Wagner, S.L., Younkin, S.G., Borchelt, D.R., 2004. Mutant presenilins specifically elevate the levels of the 42 residue beta-amyloid peptide in vivo: evidence for augmentation of a 42-specific gamma secretase. Hum. Mol. Genet. 13, 159–170.

Jankowsky, J.L., Slunt, H.H., Ratovitski, T., Jenkins, N.A., Copeland, N.G., Borchelt, D.R., 2001. Co-expression of multiple transgenes in mouse CNS: a comparison of strategies. Biomol. Eng. 17, 157–165.

Kaufer, D.I., Cummings, J.L., Christine, D., Bray, T., Castellon, S., Masterman, D., MacMillan, A., Ketchel, P., DeKosky, S.T., 1998. Assessing the impact of neuropsychiatric symptoms in Alzheimer's disease: the neuropsychiatric inventory caregiver distress scale. J. Am. Geriatr. Soc. 46, 210–215.

Kempf, S.J., Metaxas, A., Ibanez-Vea, M., Darvesh, S., Finsen, B., Larsen, M.R., 2016. An integrated proteomics approach shows synaptic plasticity changes in an APP/PS1 Alzheimer's mouse model. Oncotarget 7, 33627–33648.

Kim, I.H., Racz, B., Wang, H., Burianek, L., Weinberg, R., Yasuda, R., Wetsel, W.C., Soderling, S.H., 2013. Disruption of Arp2/3 results in asymmetric structural plasticity of dendritic spines and progressive synaptic and behavioral abnormalities. J. Neurosci. 33, 6081–6092.

Koppel, J., Acker, C., Davies, P., Lopez, O.L., Jimenez, H., Azose, M., Greenwald, B.S., Murray, P.S., Kirkwood, C.M., Kofler, J., Sweet, R.A., 2014a. Psychotic Alzheimer's disease is associated with gender-specific tau phosphorylation abnormalities. Neurobiol. Aging 35, 2021–2028.

Koppel, J., Goldberg, T.E., Gordon, M.L., Huey, E., Davies, P., Keehlisen, L., Huet, S., Christen, E., Greenwald, B.S., 2012. Relationships between behavioral syndromes and cognitive domains in Alzheimer disease: the impact of mood and psychosis. Am. J. Geriatr. Psychiatry 20, 994–1000.

Koppel, J., Jimenez, H., Azose, M., D'Abramo, C., Acker, C., Buthorn, J., Greenwald, B.S., Lewis, J., Lesser, M., Liu, Z., Davies, P., 2014b. Pathogenic tau species drive a psychosis-like phenotype in a mouse model of Alzheimer's disease. Behav. Brain Res. 275, 27–33.

Koppel, J., Sunday, S., Goldberg, T.E., Davies, P., Christen, E., Greenwald, B.S., 2014c. Psychosis in Alzheimer's disease is associated with frontal metabolic impairment and accelerated decline in working memory: findings from the Alzheimer's Disease Neuroimaging Initiative. Am. J. Geriatr. Psychiatry 22, 698–707.

Kushima, I., Nakamura, Y., Aleksic, B., Ikeda, M., Ito, Y., Shiino, T., Okochi, T., Fukuo, Y., Ujike, H., Suzuki, M., Inada, T., Hashimoto, R., Takeda, M., Kaibuchi, K., Iwata, N., Ozaki, N., 2010. Resequencing and association analysis of the KALRN and EPHB1 genes and their contribution to schizophrenia susceptibility. Schizophr. Bull. 38, 552–560.

Lalonde, R., Fukuchi, K., Strazielle, C., 2012. APP transgenic mice for modelling behavioural and psychological symptoms of dementia (BPSD). Neurosci. Biobehav. Rev. 36, 1357–1375.

Lalonde, R., Kim, H.D., Maxwell, J.A., Fukuchi, K., 2005. Exploratory activity and spatial learning in 12-month-old APP(695)SWE/co+PS1/DeltaE9 mice with amyloid plaques. Neurosci. Lett. 390, 87–92.

Laurén, J., Gimbel, D., Nygaard, H., Gilbert, J., St rittmatter, S., 2009. Cellular prion protein mediates impairment of synaptic plasticity by amyloid-beta oligomers. Nature 457, 1128–1132.

Liu, Y., Yoo, M.J., Savonenko, A., Stirling, W., Price, D.L., Borchelt, D.R., Mamounas, L., Lyons, W.E., Blue, M.E., Lee, M.K., 2008. Amyloid pathology is associated with progressive monoaminergic neurodegeneration in a transgenic mouse model of Alzheimer's disease. J. Neurosci. 28, 13805–13814.

Lopez, O.L., Becker, J.T., Sweet, R.A., Klunk, W., Kaufer, D.I., Saxton, J., Habeych, M., DeKosky, S.T., 2003. Psychiatric symptoms vary with the severity of dementia in probable Alzheimer's disease. J. Neuropsychiatry Clin. Neurosci. 15, 346–353.

Lopez, O.L., Wisniewski, S.R., Becker, J.T., Boller, F., DeKosky, S.T., 1999. Psychiatric medication and abnormal behavior as predictors of progression in probable Alzheimer disease. Arch. Neurol. 56, 1266–1272.

McCool, M.F., Varty, G.B., Del Vecchio, R.A., Kazdoba, T.M., Parker, E.M., Hunter, J.C., Hyde, L.A., 2003. Increased auditory startle response and reduced prepulse inhibition of startle in transgenic mice expressing a double mutant form of amyloid precursor protein. Brain Res. 994, 99–106.

Moyer, C.E., Erickson, S.L., Fish, K.N., Thiels, E., Penzes, P., Sweet, R.A., 2016. Developmental trajectories of auditory cortex synaptic structures and gap-prepulse inhibition of acoustic startle between early adolescence and young adulthood in mice. Cereb. Cortex 26, 2115–2126.

Mukaetova-Ladinska, E.B., Harrington, C.R., Xuereb, J., Roth, M., Wischik, C.M., 1995. Biochemical, Neuropathological, and Clinical Correlations of Neurofibrillary Degeneration in Alzheimer's Disease. Springer, New York, pp. 57–80.

Murray, P.S., Kirkwood, C.M., Gray, M.C., Fish, K.N., Ikonomovic, M.D., Hamilton, R.L., Kofler, J.K., Klunk, W.E., Lopez, O.L., Sweet, R.A., 2014a. Hyperphosphorylated tau is elevated in Alzheimer's disease with psychosis. J. Alzheimers. Dis. 39, 759–773.

Murray, P.S., Kirkwood, C.M., Gray, M.C., Ikonomovic, M.D., Paljug, W.R., Abrahamson, E.E., Henteleff, R.A., Hamilton, R.L., Kofler, J.K., Klunk, W.E., Lopez, O.L., Penzes, P., Sweet, R.A., 2012. beta-Amyloid 42/40 ratio and kalirin expression in Alzheimer disease with psychosis. Neurobiol. Aging 33, 2807–2816.

Murray, P.S., Kumar, S., DeMichele-Sweet, M.A., Sweet, R.A., 2014b. Psychosis in Alzheimer's disease. Biol. Psychiatry 75, 542–552.

Nakamura, F., 2013. FilGAP and its close relatives: a mediator of Rho-Rac antagonism that regulates cell morphology and migration. Biochem. J. 453, 17–25.

Nguyen, T.V., Galvan, V., Huang, W., Banwait, S., Tang, H., Zhang, J., Bredesen, D.E., 2008. Signal transduction in Alzheimer disease: p21-activated kinase signaling requires C-terminal cleavage of APP at Asp664. J. Neurochem. 104, 1065–1080.

Nicoll, A.J., Panico, S., Freir, D.B., Wright, D., Terry, C., Risse, E., Herron, C.E., O'Malley, T., Wadsworth, J.D., Farrow, M.A., Walsh, D.M., Saibil, H.R., Collinge, J., 2013. Amyloid-beta nanotubes are associated with prion proteindependent synaptotoxicity. Nat. Commun. 4, 2416.

Paulsen, J.S., Ready, R.E., Stout, J.C., Salmon, D.P., Thal, L.J., Grant, I., Jeste, D.V., 2000. Neurobehaviors and psychotic symptoms in Alzheimer's disease. J. Int. Neuropsychological Soc. 6, 815–820.

Perez-Madrinan, G., Cook, S.E., Saxton, J.A., Miyahara, S., Lopez, O.L., Kaufer, D.I., Aizenstein, H.J., DeKosky, S.T., Sweet, R.A., 2004. Alzheimer disease with psychosis: excess cognitive impairment is restricted to the misidentification subtype. Am. J. Geriatr. Psychiatry 12, 449–456.

Pype, S., Moechars, D., Dillen, L., Mercken, M., 2003. Characterization of amyloid beta peptides from brain extracts of transgenic mice overexpressing the London mutant of human amyloid precursor protein. J. Neurochem. 84, 602–609.

Rabiner, C.A., Mains, R.E., Eipper, B.A., 2005. Kalirin: a dual Rho guanine nucleotide exchange factor that is so much more than the sum of its many parts. Neuroscientist 11, 148–160.

Reiserer, R.S., Harrison, F.E., Syverud, D.C., McDonald, M.P., 2007. Impaired spatial learning in the APPSwe + PSEN1DeltaE9 bigenic mouse model of Alzheimer's disease. Genes Brain Behav. 6, 54–65.

Rejeb, I., Saillour, Y., Castelnau, L., Julien, C., Bienvenu, T., Taga, P., Chaabouni, H., Chelly, J., Ben Jemaa, L., Bahi-Buisson, N., 2008. A novel splice mutation in PAK3 gene underlying mental retardation with neuropsychiatric features. Eur. J. Hum. Genet. 16, 1358–1363.

Roberson, E.D., Scearce-Levie, K., Palop, J.J., Yan, F., Cheng, I.H., Wu, T., Gerstein, H., Yu, G.Q., Mucke, L., 2007. Reducing endogenous tau ameliorates amyloid beta-induced deficits in an Alzheimer's disease mouse model. Science 316, 750–754.

Ropacki, S.A., Jeste, D.V., 2005. Epidemiology of and risk factors for psychosis of Alzheimer's disease: a review of 55 studies published from 1990 to 2003. Am. J. Psychiatry 162, 2022–2030.

Rubio, M.D., Haroutunian, V., Meador-Woodruff, J.H., 2012. Abnormalities of the Duo/Ras-related C3 botulinum toxin substrate 1/p21-activated kinase 1 pathway drive myosin light chain phosphorylation in frontal cortex in schizophrenia. Biol. Psychiatry 71, 906–914.

Schneider, L.S., Dagerman, K., Insel, P.S., 2006. Efficacy and adverse effects of atypical antipsychotics for dementia: meta-analysis of randomized, placebo-controlled trials. Am. J. Geriatr. Psychiatry 14, 191–210.

Schneider, L.S., Dagerman, K.S., Insel, P., 2005. Risk of death with atypical antipsychotic drug treatment for dementia: meta-analysis of randomized placebo-controlled trials. JAMA 294, 1934–1943.

Sweet, R.A., Bennett, D.A., Graff-Radford, N.R., Mayeux, R., 2010. Assessment and familial aggregation of psychosis in Alzheimer's disease from the National Institute on Aging Late Onset Alzheimer's Disease Family Study. Brain 133, 1155–1162.

Sweet, R.A., Nimgaonkar, V.L., Devlin, B., Lopez, O.L., DeKosky, S.T., 2002. Increased familial risk of the psychotic phenotype of Alzheimer disease. Neurology 58, 907–911.

Swerdlow, N.R., Geyer, M.A., 1998. Using an animal model of deficient sensorimotor gating to study the pathophysiology and new treatments of schizophrenia. Schizophr. Bull. 24, 285–301.

Vadlamudi, R.K., Li, F., Barnes, C.J., Bagheri-Yarmand, R., Kumar, R., 2004. p41-Arc subunit of human Arp2/3 complex is a p21-activated kinase-1-interacting substrate. EMBO Rep. 5, 154–160.

van Groen, T., Kiliaan, A.J., Kadish, I., 2006. Deposition of mouse amyloid beta in human APP/PS1 double and single AD model transgenic mice. Neurobiol. Dis. 23, 653–662.

Vilalta-Franch, J., Lopez-Pousa, S., Turon-Estrada, A., Lozano-Gallego, M., Hernandez-Ferrandiz, M., Pericot-Nierga, I., Garre-Olmo, J., 2010. Syndromic association of behavioral and psychological symptoms of dementia in Alzheimer disease and patient classification. Am. J. Geriatr. Psychiatry 18, 421–432.

Wang, H., He, J., Zhang, R., Zhu, S., Wang, J., Kong, L., Tan, Q., Li, X.M., 2012. Sensorimotor gating and memory deficits in an APP/PS1 double transgenic mouse model of Alzheimer's disease. Behav. Brain Res. 233, 237–243.

Wang, P.L., Niidome, T., Akaike, A., Kihara, T., Sugimoto, H., 2009. Rac1 inhibition negatively regulates transcriptional activity of the amyloid precursor protein gene. J. Neurosci. Res. 87, 2105–2114.

Weamer, E.A., DeMichele-Sweet, M.A., Cloonan, Y.K., Lopez, O.L., Sweet, R.A., 2016. Incident psychosis in mild cognitive impairment and Alzheimer's disease subjects. J. Clin. Psychiatry 77, e1564–e1569.

Zhao, L., Ma, Q.L., Calon, F., Harris-White, M.E., Yang, F., Lim, G.P., Morihara, T., Ubeda, O.J., Ambegaokar, S., Hansen, J.E., Weisbart, R.H., Teter, B., Frautschy, S.A., Cole, G.M., 2006. Role of p21-activated kinase pathway defects in the cognitive deficits of Alzheimer disease. Nat. Neurosci. 9, 234–242.